Available online at www.sciencedirect.com

jmr&t
Journal of Materials Research and Technology
www.jmrt.com.br

Original Article

Ultrasonic cavitation assisted deposition of catalytically active metals on nitrogen-doped and non-doped carbon nanotubes — A comparative study

László Vanyorek[a,*], Ádám Prekob[a], Viktória Hajdu[a], Gábor Muránszky[a], Béla Fiser[a,b], Emőke Sikora[a], Ferenc Kristály[c], Béla Viskolcz[a]

[a] Institute of Chemistry, University of Miskolc, 3515 Miskolc-Egyetemváros, Hungary
[b] Ferenc Rákóczi II Transcarpathian Hungarian Institute, 90200 Beregszász, Transcarpathia, Ukraine
[c] Institute of Mineralogy and Geology, University of Miskolc, 3515 Miskolc-Egyetemváros, Hungary

ARTICLE INFO

Article history:
Received 10 January 2020
Accepted 14 February 2020
Available online 29 February 2020

Keywords:
Palladium
Adsorption
Nitrogen doped
Carbon nanotubes

ABSTRACT

By applying ultrasonic cavitation, palladium particles were deposited onto the surface of two different types of carbon nanotubes (nitrogen-doped bamboo-shaped carbon nanotubes, N-BCNT and multiwalled carbon nanotubes, MWCNT). To achieve this, palladium ions have been reduced by the adsorbent (N-BCNT or MWCNT) itself. Hydroxyl functional groups were identified on the surface of the MWCNTs, while amine groups have been found on the N-BCNTs. The Zeta potential was lower (−9.8 mv) in the case of the N-BCNT sample, than for MWCNT (−6.1 mV), which was in accordance with their different dispersibility in aqueous phase. The incorporated nitrogen atoms and their oxidized forms within the N-BCNT structure lead to increased adsorption capacity and thus, this type of nanotube is more efficient adsorbent for Pd particles, than MWCNT. The higher adsorption capacity of the N-BCNTs can be explained by the presence of nitrogen atoms which increase the interaction between the Pd and nanotubes. Both Pd/nanotube systems show high catalytic activity (after 30 min – 99% aniline yield) in hydrogenation of nitrobenzene to aniline. Thus, palladium coated carbon nanotubes were synthetized in a one-step reduction procedure, and the produced composites are applicable as catalysts in heterogeneous hydrogenation reactions.

1. Introduction

Carbon nanomaterials have a wide range of application such as electromagnetic wave shielding [1,2], storage systems [3,4], sensor production [5,6], and composite material (and coating) preparation [7–10].

* Corresponding author.
E-mail: kemvanyi@uni-miskolc.hu (L. Vanyorek).
https://doi.org/10.1016/j.jmrt.2020.02.054

Carbon nanotubes are widely used and important carbon materials which are applicable as catalyst support materials. Several different precious metals (e.g. palladium, platinum, iridium and rhodium) could serve as catalysts and be supported by nanotubes and these complex nanotube-metal systems can be applied successfully in various hydrogenation reactions (nitrobenzene, nitrocyclohexene, cinnamaldehyde, carbon dioxide) and Fischer–Tropsch synthesis as well [11–16]. Various features (e.g. lifetime) of the catalysts can be improved by taking advantage of the strong adsorption interactions between the catalytically active metals and the nanotubes applied as support materials [7–17].

On the surface of the nanotubes, the formation of carboxyl and hydroxyl functional groups can be induced by oxidative treatment and these chemically modified structures are good candidates for heavy metal adsorption [28–30]. A widely accepted view is that the surface modification is inevitable to achieve suitable adsorption, because the ion exchange and complexation depends on the functional groups located on the exterior of the materials [18,20,25]. The presence of dissociable functional groups (indicated with negative Zeta potential) can help to stabilize the aqueous dispersion of carbon nanotubes (CNTs). However, these oxidized CNTs are not recommended as catalyst supports in non-polar reaction media (e.g. liquid phase hydrogenation processes). In our recent study [31], the activity of palladium containing oxidized carbon nanotube supported catalysts have been compared with their non-oxidized counterparts during octadecene hydrogenation in a non-polar solvent (octanol). The oxidative treatment decreased the catalytic activity and thus, the best results were achieved by the non-oxidized CNT supported sample. Therefore, it may be expedient to omit oxidative pretreatments during catalyst preparation. Instead of those, in-situ functionalization can be performed by incorporating different heteroatoms (e.g. nitrogen doping) into the structure of the nanotubes during the CCVD synthesis [32]. Doping already have many useful applications according to the literature [33–35]. These heteroatom-containing structures (e.g. nitrogen-doped carbon nanotubes, N-CNTs) have high adsorption potential [26,27] extraordinary electronic and structural properties (e.g. bamboo-shaped structure), and enhanced reactivity as plenty of accessible interaction points appeared on their surface [21–24] without dealing with the disadvantages of oxidative treatment. However, if it is necessary these can still be treated oxidatively and the enhanced reactivity of their interaction sites will increase the formation of oxygen containing functional groups which will also serve as adsorption anchor points on the structure. Partial oxidation of the N-CNTs could happen during the synthesis and purification procedure, thus further oxidative treatment can be avoided. In case of the nitrogen-doped carbon nanotubes, the high heavy metal adsorption capacity is related to the presence of heteroatoms in the system [19]. The anchoring of metal ions on the surface of adsorbents, can be increased by acoustic cavitation, which helps the formation of nanoparticles from metal ions (for example catalytic metals ions). In this sense, the cavitation supported metal-adsorption is applicable as a catalyst preparation process. During ultrasound irradiation of liquids vapour microbubbles will form. These microbubbles will collapse, because of the higher pressure of their environment. In the microvolumes of the collapsed bubbles an intense local heating and high pressure generated, and this volume is the so called hot spot. The high energy of the "hot spots" more than enough to form metal and metal-oxide nanoparticles from their precursors in presence of a reducing agent [36]. In this work, nitrogen-doped bamboo-shaped carbon nanotubes and their non-doped counterparts, multi-walled carbon nanotubes (MWCNTs) have been studied and compared in terms of their precious metal adsorption potential. The results have been employed in catalyst development and a simplified catalyst preparation method was developed by applying ultrasound activation. Palladium coated carbon nanotubes were synthetized in a one-step reduction procedure, within which the adsorbent (N-BCNT or MWCNT) reduced the metal ions to metals. The final Pd/nanotube composite materials are applicable in heterogeneous catalysis, because the palladium is deposited in a catalytically active form onto the surface of the nanotubes, and further activation is not necessary. Thus, a simplified catalyst preparation procedure is achieved.

2. Experimental sections

2.1. Materials

Butylamine (VWR), and acetylene (Messer) were used as carbon source during the synthesis of nanotubes. Nickel-nitrate hexahydrate ($Ni(NO_3)_6{*}6H_2O$, Sigma Aldrich), cobalt(II)–nitrate hexahydrate ($Co(NO_3)_2{*}6H_2O$, Reanal), iron(III)–nitrate nonahydrate ($Fe(NO_3)_3{*}9H_2O$, Sigma Aldrich), magnesium-oxide (Reanal), and Patosolv (mixture of aliphatic alcohols, Molar Chem.) were applied for the preparation of catalysts used in the catalytic chemical vapor deposition (CCVD) method. The adsorption capacity of the nanotubes have been tested by using palladium-nitrate dihydrate ($Pd(NO_3)_2{*}2H_2O$, Aldrich).

2.2. Synthesis of the nanotubes (MWCNTs and N-BCNTs)

The synthesis of MWCNTs was carried out at 700 °C within 30 min by using 2.5 g catalyst (2.5 wt% Co and 2.5 wt% Fe on MgO support) in a CCVD procedure. Acetylene was applied as carbon source and nitrogen as carrier gas (C_2H_2:N_2, 1:10). To prepare N-BCNTs also the CCVD method was applied, but in this case the reaction was carried out within 20 min at 650 °C, and the carbon source was *n*-butylamine (total amount 4.00 g), while the catalyst was 5 wt% Ni/MgO (2.5 g). The remnant catalysts were removed from the nanotube samples by using hydrochloride acid solution (36 wt%), and the purity of the final product was monitored by thermogravimetric analysis (TGA).

2.3. Adsorption tests of the carbon nanotubes

To measure and compare the adsorption potential of the CNT samples, 10 mg nanotubes were added to 50 ml Pd^{2+} solution in each case. The metal ion concentration was varied between

0.025–0.25 mmol dm^{-3}, with 0.05 increment. The dispersions were homogenized by Hielscher UIP1000hdT type homogenizer at 75 W for 10 min. After 90 min of contact time, all dispersions were filtered. The change in the metal ion concentrations was measured by using a Varian 720 ES inductively coupled optical emission spectrometer (ICP-OES).

2.4. Catalytic tests of the palladium/CNT samples in hydrogenation of nitrobenzene

The nitrobenzene hydrogenation was carried out at 20 bar hydrogene pressure and 323 K temperature in Büchi Uster Picoclave (Volume: 150 cm^3) reactor system. The weight of the Pd/CNT samples was 100 mg in each case, which was added to the methanol based solution of nitrobenzene (c = 0.25 mol/dm^3), and the mixing speed was 1000 min^{-1}. Sampling took place after the beginning of hydrogenation at 0, 5, 10, 20, 30, 60, 120, and 180 minutes. The separation was performed on RTX-624 column (60 m × 0.25 mm x1.4 μm). The injected sample volume was 1 μL at 200:1 split ratio, while the inlet temperature was set to 473 K. The carrier gas was helium with constant flow (2.28 mL/min), and the oven temperature was set to 323 K for 3 min. Then, it was heated up to 523 K with 10 K/min increments and kept there for another 3 min.

2.5. Characterization methods

The morphology of the nanotubes was characterized by using a Fei Technai G2 high resolution transmission electron microscope (HRTEM) with 200 kV acceleration voltage. During the sample preparation aqueous dispersions of CNTs were dropped onto carbon coated copper grids (Ted Pella, 300 mesh).

Surface areas were measured volumetrically by applying a Micromeritics ASAP 2020 equipment. Nitrogen adsorption was performed at 77 K (in liquid nitrogen bath), and analyzed based on the Brunauer–Emmett–Teller (BET) theory.

X-ray diffraction (XRD) measurements were used to identify and quantify the crystalline phases of the palladium. Bruker D8 Advance diffractometer (Cu-Kα source, 40 kV and 40 mA) in a parallel beam geometry (Göbel mirror) with Vantec1 detector was applied to perform the XRD measurements. The functional groups on the surface of the oxidized carbon nanotubes were determined by Bruker Vertex 70 Fourier-transform infrared spectroscope (FTIR). All samples were investigated in potassium–bromide pellets (5 mg N-BCNT in 250 mg KBr). The oxidized samples have been studied by X-ray photoelectron spectroscopy (SPECS spectroscope with Phoibos 150 MCD analyzer) to identify the type of nitrogen incorporation. Electro-kinetic potential measurements were carried out by using a Malvern Nano Zs equipment, and the electrophoretic mobility was determined by using the Smoluchowski equation. Concentration of the precious metal solutions were analyzed by using a Varian 720 ES inductively coupled optical emission spectrometer (ICP-OES) in combination with the Merck Certipur ICP multi-element standard IV.

3. Results and discussion

3.1. Characterization of the nanotubes

The purified carbon nanotube samples were studied by high-resolution transmission electron microscopy (HRTEM). There are several structural differences between the two types of nanotubes which are clearly visible on the HRTEM images (Fig. 1A–F) and caused by the incorporation of nitrogen atoms into the N-BCNTs. The catalytically active metals, applied during the CCVD synthesis, prefer to bind nitrogen over carbon atoms (metal-N > metal-C), which distracts the nanotube formation mechanism and lead to the formation of nitrogen-doped bamboo-shaped carbon nanotubes (N-BCNT) [37]. The edges of the bamboo-shaped structure are full of potential anchor points for metal ions, because it contains sp^3 hybridized carbon atoms decorated with amine, hydroxyl and carboxyl groups. The purity of the carbon nanotubes was determined by TGA measurements. The total carbon content was 95.9 w% and 98.4 wt% for MWCNTs and N-BCNTs, respectively (SI Fig. 1). The BET surface area based on N_2 adsorption/desorption measurements was 90.7 m^2/g and 96.4 m^2/g for N-BCNTs, and for MWCNTs, respectively.

X-ray photoelectron spectroscopy (XPS) have been used to identify the nitrogen incorporation types in the N-BCNTs. Three different types of nitrogen were identified: pyridinic, graphitic and oxidized nitrogen (Fig. 2). The pyridinic and graphitic were found on the deconvoluted N1s band of the N-BCNT sample at 398.4 eV and 401.1 eV binding energy, respectively (Fig. 2A). From a structural point of view, pyridinic nitrogen atoms could serve as adsorption sites for metal ions (Fig. 2B). The adsorption potential of graphitic or quaternary nitrogen atoms (nitrogen replace carbon in the graphitic structure, Fig. 2C) is lower compare to the pyridinic N atoms. The peak around 404.9 eV corresponds to the oxidized nitrogen (pyridine N–oxide, N—O^-) species and the so-called shake-up satellites have also identified around 408 eV [32]. The pyridine N-O- species increase the negative charge of the N-BCNT surface and serves as additional anchor points for the metal ions (Fig. 2D). Two additional peaks were identified at higher binding energies (on the deconvoluted O1s band), which are attributed to the presence of surface hydroxyl and carboxyl groups (Fig. 2E). The peaks (532.7 eV and 530.9 eV) can be assigned to the C—O (C—OH groups) and C=O bonds, as well as the —COOH groups, respectively.

The nanotubes were also examined by Fourier-transform infrared spectroscopy (Fig. 3A). Different structural moieties have been identified in the nanotubes by assigning them to the peaks which are appeared on the FTIR spectra. Two peaks emerged at ~1140 and ~1220 cm^{-1} wavenumbers which indicates the stretching of C—O bonds [38–40]. In case of N-BCNTs, C-N bonds have been formed in the walls of the nanotubes and it was confirmed by a maximum at 1189 cm^{-1}. The adsorption peaks are attributed to the C=C bands at 1582 and 1586 cm^{-1} on the spectra of both CNTs, which corresponds to the vibration of the lattice structure of the carbon nanotubes. Wavenumbers of 1705 cm^{-1} and 1701 cm^{-1} correspond to carboxyl (COOH) groups. The peaks around 2820 cm^{-1} and 2890 cm^{-1} are attributed to the symmetric and asymmetric

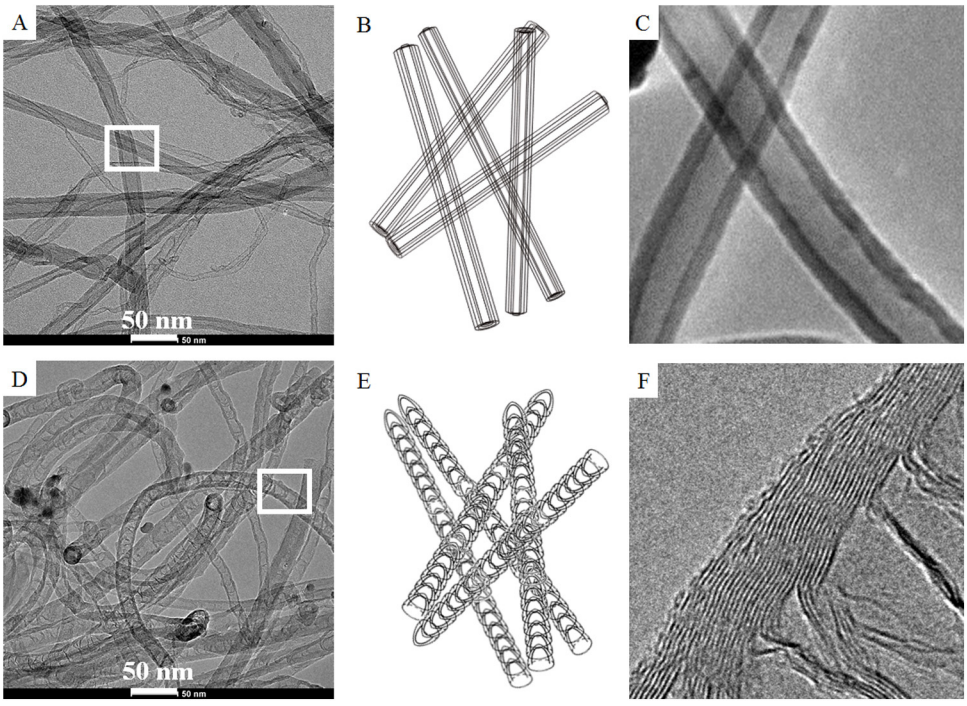

Fig. 1 – HRTEM images of the non-doped multi-walled carbon nanotubes (MWCNTs, A, C-section), nitrogen-doped bamboo-shaped carbon nanotubes (N-BCNTs, D, F-section), and schematic illustrations of the structures ((B) - MWCNT, and (E) - N-BCNT). C and F are cut-out sections of A and D, respectively, which are highlighted by white frames on the original images.

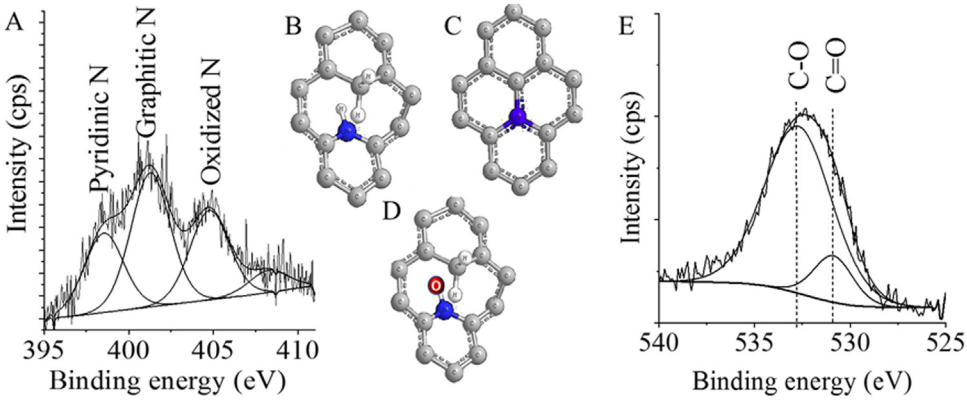

Fig. 2 – XPS spectra of the N-BCNT sample (A), and structural representations of the identified nitrogen incorporations: pyridinic (B), graphitic (C) and oxidized (D) nitrogen atoms, and the deconvoluted O1s band (E).

C—Hx stretching vibration. Intensive peaks at 3455 cm^{-1} and 3414 cm^{-1} are indicates the presence of –OH groups in both nanotubes [38–40]. The surface functional groups of the carbon nanotube samples were also examined by XPS (Fig. 3B and C). The XPS results confirmed the presence of those functional groups, which were detected by FTIR. On the deconvoluted C 1s bands of the nanotubes a peak at 284.5 eV binding energy has been found which is corresponds to the C-C bonds. The C=O bonds of the carboxyl groups resulted adsorption maximum at 287.5 eV and 287.2 eV. The C—O bonds are visible at 291.2 eV and 290.6 eV. The last peaks after 294 eV correspond to the "shake up" satellite [32].

The Zeta potential (ζ) of the aqueous dispersion of N-BCNT was more negative (ζ = −9.8 mV) and thus, it is formed a more stable dispersion than the MWCNT (ζ = −6.1 mv) (Fig. 4B and C). The presence of pyridine N-oxide groups (negative surface charge) could be one of the reasons behind the enhanced dispersibility of N-BCNT in water. The electronegative heteroatom (nitrogen) incorporation increase the polar character, which also leads to enhanced wettability (Fig. 4B).

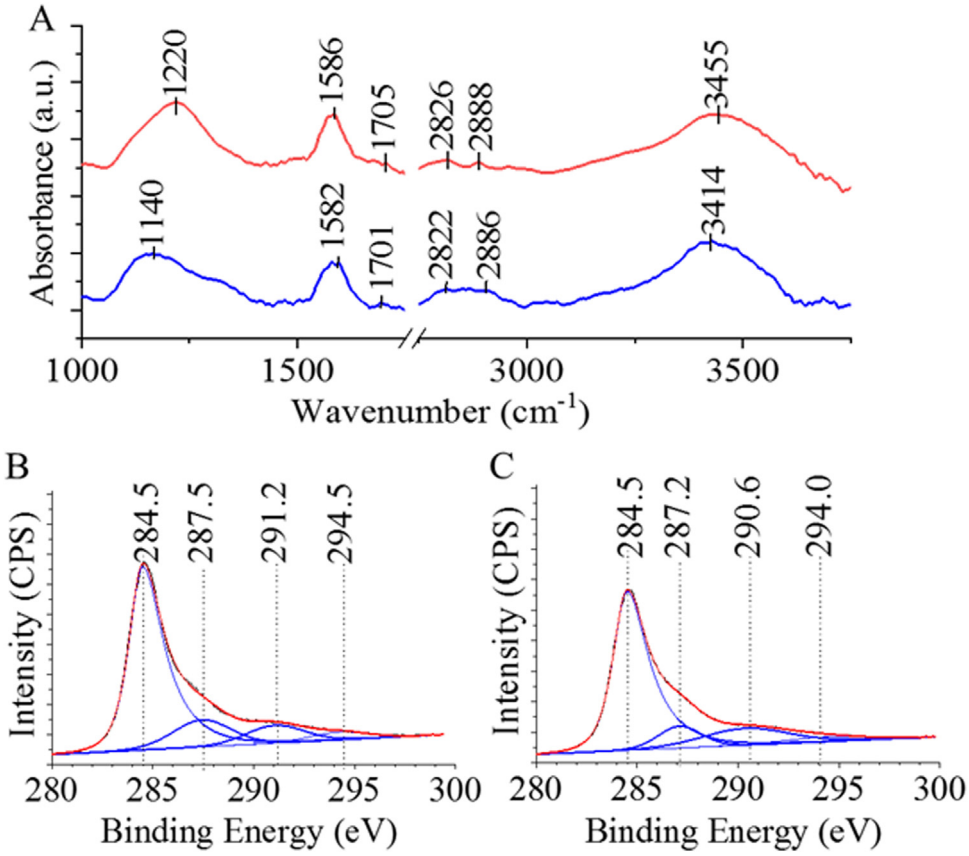

Fig. 3 – FTIR spectra of the MWCNT (red line) and N-BCNT (blue line) samples (A). XPS spectrum, C 1 s bands of the MWCNT (B) and N-BCNT (C).

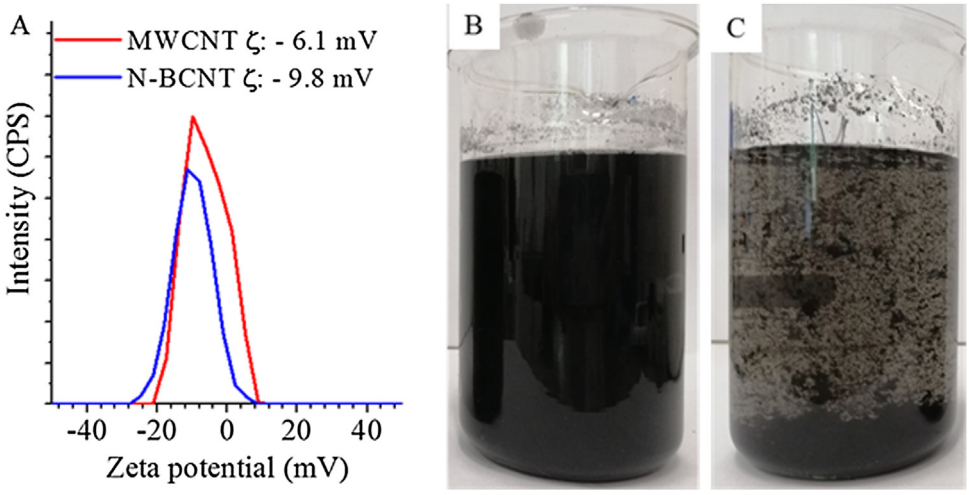

Fig. 4 – Zeta potential distribution of carbon nanotubes (A), aqueous dispersion of the N-BCNTs (B) and MWCNTs (C).

3.2. *Analysis of the palladium phases on the carbon nanotubes*

Reflexion peaks of elemental palladium, and palladium-hydride can be identified on the XRD spectrum of the Pd/N-BCNT composite (Fig. 5A). Thus, the palladium ions were reduced to elemental palladium (Pd°) during the synthetic procedure. In case of the MWCNT, besides the palladium (JCPDS 46-1043), PdO_X phases have also identified. It can be formed by O insertion into the cubic structure of metal to yield a non-stochiometric palladium oxide [41]. Furthermore, the stociometric PdO phase (JCPDS. 41-1107) have been also determined (Fig. 5B). The reduction of Pd ions was not complete in case of MWCNT. Magnesium oxide (JCPDS 04-009-5447) has also been found in the Pd/MWCNT system, which is remained from the catalyst of the CCVD synthesis.

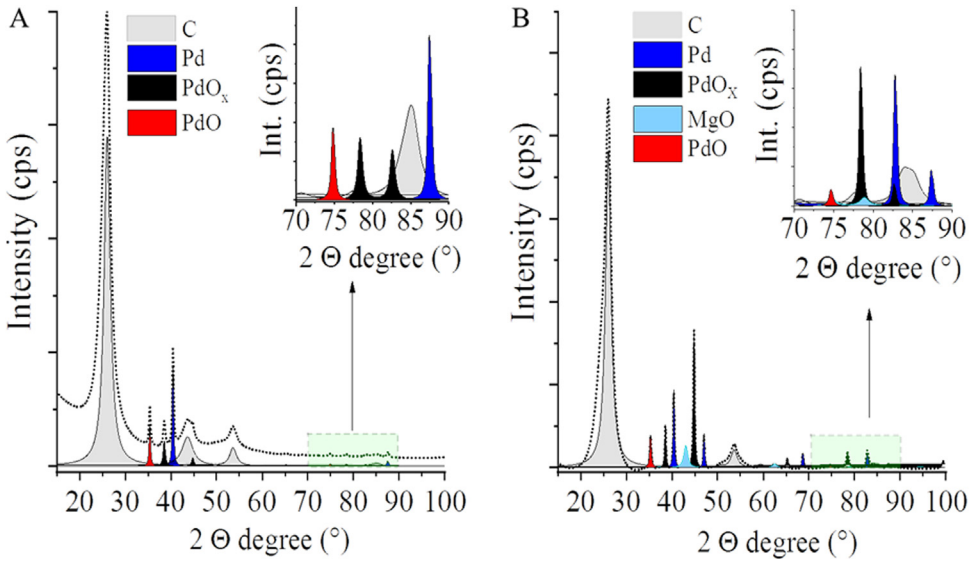

Fig. 5 – Deconvoluted XRD spectra of Pd/N-BCNT (A) and Pd/MWCNT (B) composites.

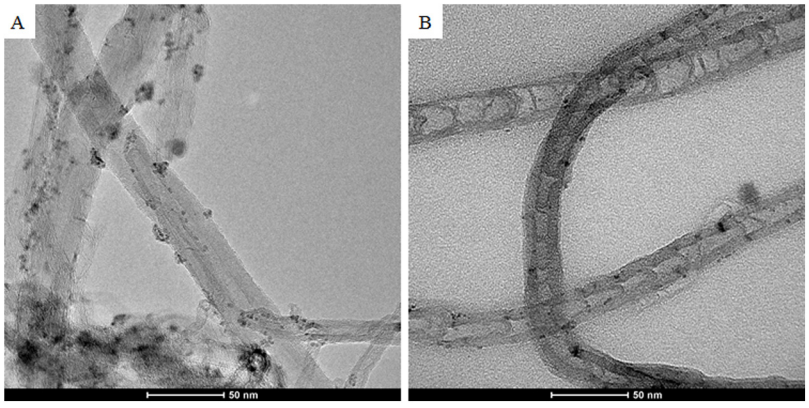

Fig. 6 – HRTEM image of the Pd/MWCNT (A) and Pd/N-BCNT (B) system.

HRTEM images were made from the carbon nanotubes after adsorption of palladium. The average diameter of Pd nanoparticles on the surface of the nanotubes is very small, 2.7 nm and 3.1 nm for N-BCNT and MWCNT, respectively (Fig. 6A and B).

During ultrasound irradiation of liquids vapour microbubbles will form. These microbubbles will collapse, because of the higher pressure of their environment. In the microvolumes of the collapsed bubbles an intense local heating and high pressure generated, and this volume is the so-called hot spot. The high energy of the, hot spots" more than enough to form metal and metal–oxide nanoparticles from their precursors in presence of a reducing agent.

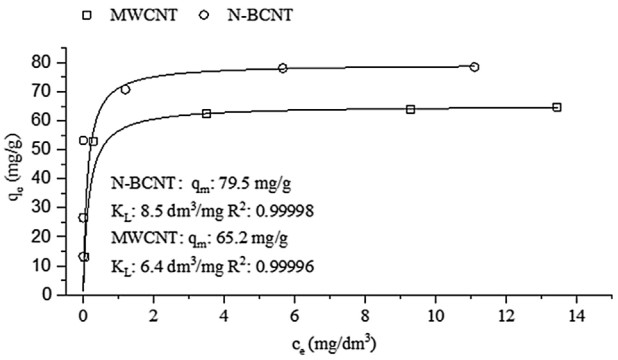

Fig. 7 – Adsorption of palladium on MWCNT and N-BCNT.

3.3. *Adsorption capacity of the nanotubes*

Langmuir isotherm model was used to characterize the adsorption mechanism, and the data were plotted according to the Langmuir equation:

$$q_e = \frac{q_m \times K_L \times c_e}{1 + c_e \times K_L}$$

where q_e is the amount of adsorbed Pd (mg/g), Ce is the equilibrium concentration of the precious metal ions in the solution (mg/dm^3), q_m is the maximum sorption capacity (mg/g), and K_L is the Langmuir equilibrium constant (dm^3/mg). K_L and q_m were calculated with nonlinear regression, by using the slope and intercept of the curves (Fig. 7). The correlation coefficient

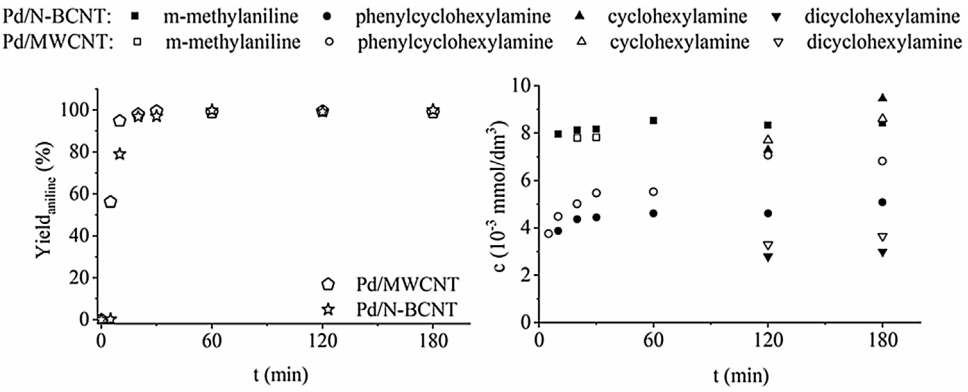

Fig. 8 – Yield of aniline (A) and concentration of the by-products (B) over time of hydrogenation in case of the Pd/N-BCNT and Pd/MWCNT catalysts.

Table 1 – Gibbs free energy change of adsorption (ΔG°_{ads}).

	N-BCNT	MWCNT
Pd	$\Delta G^\circ_{ads.} = -44.0$ kJ/mol	$\Delta G^\circ_{ads.} = -43.2$ kJ/mol

was high in each case, which indicates that the adsorption follows the Langmuir model. The maximum amount of adsorbed palladium was 79.5 mg/g on N-BCNTs and 65.2 mg/g in case of MWCNTs (Fig. 7). The adsorbed quantity of the Pd (~8 wt% and 6.5 wt%) is enough to reach suitable catalytic behavior with the impregnated CNTs (Pd content generally around 5 wt% in case of the commercial carbon supported catalysts). The Zeta potential of both carbon nanotubes is negative, thus, the adsorption of an electropositive metal on the nanotubes is preferred. The adsorption mechanism also affected by the complex formation between palladium and the incorporated nitrogen atoms in case of N-BCNT. The nitrogen incorporation weakens the π–π interaction between the neighboring carbon atoms, thus the metal ions (palladium) can establish donor-acceptor interaction with the π-system of N-BCNTs.

The Langmuir constant was higher ($K_L = 8.5$ dm^3/mg) by using Pd^{2+} precursor, in case of N-BCNT, compare to MWCNT ($K_L = 6.4$ dm^3/mg). The increased K_L can be attributed to the stronger interaction between the palladium and N-BCNT. The Gibbs free energy change (ΔG°) indicates the degree of spontaneity of an adsorption process, and a higher negative value reflects a more energetically favorable adsorption. The ΔG° of adsorption was calculated in case of the two types of carbon nanotubes, based on the following equation [42]:

$$\Delta G^\circ_{ads.} = -R \times T \times \ln\left(\frac{K_L \times M_{Pd}}{V_m}\right)$$

In case of the N-BCNT, ΔG°_{ads} is slightly more negative than in case of the MWCNT, and thus, the nitrogen-doped carbon nanotubes are more efficient adsorbents. However, ΔG°_{ads} is negative in both cases, which shows that the adsorption of the palladium on the surface of the nanotubes is spontaneous (Table 1). This confirms that the tested carbon nanotubes are efficient adsorbents for precious metals.

The increased adsorption capacity of the N-BCNTs can be explained by the possible donor-acceptor interaction between the d orbital of the metal and the disturbed π-system of the nitrogen-doped nanotube.

3.4. *Catalytic tests of the palladium/CNT systems*

Both catalysator systems were tested in hydrogenation of nitrobenzene to aniline (Fig. 8A). In both cases high catalytic activity was achieved, after 30 min the aniline yield was above 99 % (99.5 % and 99.8 % for Pd/MWCNT and Pd/N-BCNT, respectively). By-products such as *n*-methylaniline, phenyl cyclohexylamine, cyclohexylamine and dicyclohexylamine were formed in very low concentration (<0.001 mmol/dm^3) [43] (Fig. 8 B). Significant difference between the two catalysts were not found in terms of the aniline yield and the amount of the by-products. According to the hydrogenation tests, the prepared Pd/CNT systems are catalytically active and thus, the ultrasonic cavitation assisted palladium deposition (adsorption) onto the surface of carbon nanotubes is an efficient way for catalyst preparation.

4. Conclusions

Adsorption of catalytically active metal nanoparticles were compared in case of two types of carbon nanotubes, nitrogen-doped bamboo-shaped carbon nanotubes (N-BCNT) and multi-walled carbon nanotubes (MWCNT). N-BCNTs are more efficient adsorbents for palladium, than the non-doped MWCNTs. The adsorbed quantity of the palladium on the N-BCNTs and on the MWCNTs is ~8 wt% and 6.5 wt%, respectively, which is suitable to apply in catalytic processes. Thus, no further chemical treatment (e.g. functionalization) is necessary in order to achieve appropriate adsorption capacity. The Langmuir constant was higher ($K_L = 8.5$ dm^3/mg) in case of palladium adsorption on N-BCNT, than on MWCNT ($K_L = 6.4$ dm^3/mg). Thus, the interaction is stronger between the palladium and N-BCNT surface. The Gibbs free energy change of adsorption is negative in both cases, which indicates that the adsorption of palladium on the surface of the nanotubes is spontaneous. The tested carbon nanotubes are efficient adsorbents for precious metal particles. The nitrogen-doped carbon nanotubes as adsorbent for palladium are more efficient, than their non-doped counterparts due

to their electronic and structural features, which increase their adsorption capacity. All in all, palladium coated carbon nanotubes (Pd/MWCNT and Pd/N-BCNT) were synthesized in a one-step reduction procedure, within which the adsorbent reduced the metal ions, and the produced composites are applicable in heterogeneous catalysis. The two Pd/CNT systems were tested in nitrobenzene hydrogenation to produce aniline and in both cases excellent catalytic activity was achieved (after 30 min the aniline yield was above 99%). We concluded, the ultrasonic cavitation assisted palladium deposition (adsorption) onto the surface of carbon nanotubes is an efficient and simplified way for catalyst preparation.

Conflict of interest

On behalf of all authors, the corresponding author states that there is no conflict of interest.

Acknowledgements

This research was supported by the European Union and the Hungarian State, co-financed by the European Regional Development Fund in the framework of the GINOP-2.3.4-15-2016-00004 project, aimed to promote the cooperation between the higher education and the industry.

Appendix A. Supplementary data

Supplementary data associated with this article can be found, in the online version, at https://doi.org/10.1016/j.jmrt.2020.02.054.

REFERENCES

[1] Wang C, Murugadoss V, Kong J, He Z, Mai X, Shao Q, et al. Overview of carbon nanostructures and nanocomposites for electromagnetic wave shielding. Carbon 2018;140:696–733, http://dx.doi.org/10.1016/j.carbon.2018.09.006.

[2] Jiang D, Murugadoss V, Wang Y, Lin J, Ding T, Wang Z, et al. Electromagnetic interference shielding polymers and nanocomposites — a review. Polym Rev 2019;59:280–337, http://dx.doi.org/10.1080/15583724.2018.1546737.

[3] Hayashi J, Kazehaya A, Muroyama K, Watkinson AP. Preparation of activated carbon from lignin by chemical activation. Carbon 2000;38:1873–8, http://dx.doi.org/10.1016/S0008-6223(00)00027-0.

[4] Kirubasankar B, Murugadoss V, Lin J, Ding T, Dong M, Liu H, et al. In situ grown nickel selenide on graphene nanohybrid electrodes for high energy density asymmetric supercapacitors. Nanoscale 2018;10:20414–25, http://dx.doi.org/10.1039/c8nr06345a.

[5] Wei HG, Wang H, Li A, Cui DP, Zhao ZN, Chu LQ, et al. Multifunctions of polymer nanocomposites: environmental remediation, electromagnetic interference shielding, and sensing applications. ChemNanoMat 2020;6:174–84, http://dx.doi.org/10.1002/cnma.201900588.

[6] Chen J, Yu Q, Cui X, Dong M, Zhang J, Wang C, et al. An overview of stretchable strain sensors from conductive polymer nanocomposites. J Mater Chem C 2019;7:11710–30, http://dx.doi.org/10.1039/c9tc03655e.

[7] He Y, Wu D, Zhou M, Liu H, Zhang L, Chen Q, et al. Effect of MoO_3/carbon nanotubes on friction and wear performance of glass fabric-reinforced epoxy composites under dry sliding. Appl Surf Sci 2020;506:144946, http://dx.doi.org/10.1016/j.apsusc.2019.144946.

[8] Lou C, Jing T, Tian J, Zheng Y, Zhang J, Dong M, et al. 3-Dimensional graphene/Cu/Fe3O4 composites: Immobilized laccase electrodes for detecting bisphenol A. J Mater Res 2019;34:2964–75, http://dx.doi.org/10.1557/jmr.2019.248.

[9] Zhang J, Zhang W, Wei L, Pu L, Liu J, Liu H, et al. Alternating multilayer structural epoxy composite coating for corrosion protection of steel. Macromol Mater Eng 2019;304:1900374, http://dx.doi.org/10.1002/mame.201900374.

[10] Guo Y, Yang X, Ruan K, Kong J, Dong M, Zhang J, et al. Reduced graphene oxide heterostructured silver nanoparticles significantly enhanced thermal conductivities in hot-pressed electrospun polyimide nanocomposites. ACS Appl Mater Interfaces 2019;11:25465–73, http://dx.doi.org/10.1021/acsami.9b10161.

[11] Dong B, Li Y, Ning X, Wang H, Yu H, Peng F. Trace iron impurities deactivate palladium supported on nitrogen-doped carbon nanotubes for nitrobenzene hydrogenation. Appl Catal A Gen 2017;545:54–63, http://dx.doi.org/10.1016/J.APCATA.2017.07.035.

[12] Li C-H, Yu Z-X, Yao K-F, Ji S, Liang J. Nitrobenzene hydrogenation with carbon nanotube-supported platinum catalyst under mild conditions. J Mol Catal A Chem 2005;226:101–5, http://dx.doi.org/10.1016/j.molcata.2004.09.046.

[13] Liao H-G, Xiao Y-J, Zhang H-K, Liu P-L, You K-Y, Wei C, et al. Hydrogenation of nitrocyclohexane to cyclohexanone oxime over Pd/CNT catalyst under mild conditions. Catal Commun 2012;19:80–4, http://dx.doi.org/10.1016/j.catcom.2011.12.027.

[14] Liu R, Liu R, Ma X, Davis BH, Li Z. Efficient diesel production over the iron-based Fischer–Tropsch catalyst supported on CNTs treated by urea/NaOH. Fuel 2018;211:827–36, http://dx.doi.org/10.1016/j.fuel.2017.09.114.

[15] Pham-Huu C, Keller N, Ehret G, Charbonniere LJ, Ziessel R, Ledoux MJ. Carbon nanofiber supported palladium catalyst for liquid-phase reactions. J Mol Catal A Chem 2001;170:155–63, http://dx.doi.org/10.1016/S1381-1169(01)00055-3.

[16] Sikora E, Prekob Á, Halasi G, Vanyorek L, Pekker P, Kristály F, et al. Development and application of carbon-layer-stabilized, nitrogen-doped, bamboo-like carbon nanotube catalysts in CO_2 hydrogenation. ChemistryOpen 2018;7:789–96, http://dx.doi.org/10.1002/open.201800162.

[17] Chagas PMB, de Carvalho LB, Caetano AA, Nogueira FGE, Corrêa AD. Guimarães I do R. Nanostructured oxide stabilized by chitosan: hybrid composite as an adsorbent for the removal of chromium (VI). J Environ Chem Eng 2018;6:1008–19, http://dx.doi.org/10.1016/J.JECE.2018.01.026.

[18] Yang RT. Nanostructured adsorbents. Adv Chem Eng 2001;27:79–124, http://dx.doi.org/10.1016/S0065-2377(01)27004-5.

[19] Yang X, Wan Y, Zheng Y, He F, Yu Z, Huang J, et al. Surface functional groups of carbon-based adsorbents and their roles in the removal of heavy metals from aqueous solutions: a critical review. Chem Eng J 2019;366:608–21, http://dx.doi.org/10.1016/j.cej.2019.02.119.

[20] Ehsani P, Tehrani MS, Azar PA, Ehsani Namin P, Dehaghi SM. Removal of lead ions from aqueous solution using multi-walled carbon nanotubes: the effect of functionalization. J Appl Environ Biol Sci 2014;4:316–26.

[21] Li Y-H, Hung T-H, Chen C-W. A first-principles study of nitrogen- and boron-assisted platinum adsorption on carbon nanotubes. Carbon 2009;47:850–5, http://dx.doi.org/10.1016/j.carbon.2008.11.048.

[22] Zhou Z, Gao X, Yan J, Song D. Doping effects of B and N on hydrogen adsorption in single-walled carbon nanotubes through density functional calculations. Carbon 2006;44:939–47, http://dx.doi.org/10.1016/j.carbon.2005.10.016.
[23] Kumar MP, Kesavan T, Kalita G, Ragupathy P, Narayanan TN, Pattanayak DK. On the large capacitance of nitrogen doped graphene derived by a facile route. RSC Adv 2014;4:38689–97, http://dx.doi.org/10.1039/C4RA04927F.
[24] Joshi A, Nagaiah TC. Nitrogen-doped carbon nanotubes for sensitive and selective determination of heavy metals. RSC Adv 2015;5:105119–27, http://dx.doi.org/10.1039/C5RA15944J.
[25] Perez-Aguilar NV, Muñoz-Sandoval E, Diaz-Flores PE, Rangel-Mendez JR. Adsorption of cadmium and lead onto oxidized nitrogen-doped multiwall carbon nanotubes in aqueous solution: equilibrium and kinetics. J Nanopart Res 2010;12:467–80, http://dx.doi.org/10.1007/s11051-009-9670-6.
[26] Andrade-Espinosa G, Muñoz-Sandoval E, Terrones M, Endo M, Terrones H, Rangel-Mendez JR. Acid modified bamboo-type carbon nanotubes and cup-stacked-type carbon nanofibres as adsorbent materials: cadmium removal from aqueous solution. J Chem Technol Biotechnol 2009;84:519–24, http://dx.doi.org/10.1002/jctb.2073.
[27] Diaz-Flores PE, López-Urıás F, Terrones M, Rangel-Mendez JR. Simultaneous adsorption of Cd2+ and phenol on modified N-doped carbon nanotubes: experimental and DFT studies. J Colloid Interface Sci 2009;334:124–31, http://dx.doi.org/10.1016/j.jcis.2009.02.045.
[28] Ebbesen TW, Hiura H, Bisher ME, Treacy MMJ, Shreeve-Keyer JL, Haushalter RC. Decoration of carbon nanotubes. Adv Mater 1996;8:155–7, http://dx.doi.org/10.1002/adma.19960080212.
[29] Chen C-M, Chen M, Leu F-C, Hsu S-Y, Wang S-C, Shi S-C, et al. Purification of multi-walled carbon nanotubes by microwave digestion method n.d. https://doi.org/10.1016/j.diamond.2003.11.016.
[30] Wang Y, Gao L, Sun J, Liu Y, Zheng S, Kajiura H, et al. An integrated route for purification, cutting and dispersion of single-walled carbon nanotubes. Chem Phys Lett 2006;432:205–8, http://dx.doi.org/10.1016/J.CPLETT.2006.10.054.
[31] Vanyorek L, Sikora E, Kiss A, Sike Á, Hutkai ZG, Pekker P, et al. Nitrogen-doped bamboo-shaped carbon nanotube supported catalysts for heterogeneous hydrogenation. The effect of surface polarity. React Kinet Mech Catal 2018;125:37–46, http://dx.doi.org/10.1007/s11144-018-1422-0.
[32] Vanyorek L, Muranszky G, Sikora E, Pénzeli X, Prekob Á, Kiss A, et al. Synthesis optimization and characterization of nitrogen-doped bamboo-shaped carbon nanotubes. J Nanosci Nanotechnol 2019;19:429–35, http://dx.doi.org/10.1166/jnn.2019.15776.
[33] Song B, Wang Q, Wang L, Lin J, Wei X, Murugadoss V, et al. Carbon nitride nanoplatelet photocatalysts heterostructured with B-doped carbon nanodots for enhanced photodegradation of organic pollutants. J Colloid Interface Sci 2020;559:124–33, http://dx.doi.org/10.1016/j.jcis.2019.10.015.
[34] Idrees M, Batool S, Kong J, Zhuang Q, Liu H, Shao Q, et al. Polyborosilazane derived ceramics — nitrogen sulfur dual doped graphene nanocomposite anode for enhanced lithium ion batteries. Electrochim Acta 2019;296:925–37, http://dx.doi.org/10.1016/j.electacta.2018.11.088.
[35] Shi C, Qi H, Ma R, Sun Z, Xiao L, Wei G, et al. N,S-self-doped carbon quantum dots from fungus fibers for sensing tetracyclines and for bioimaging cancer cells. Mater Sci Eng C 2019;105:110132, http://dx.doi.org/10.1016/j.msec.2019.110132.
[36] Suslick K. Kirk-Othmer encyclopedia of chemical technology. 4th ed. New York: J. Wiley & Sons; 1998.
[37] O'Byrne JP, Li Z, Jones SLT, Fleming PG, Larsson JA, Morris MA, et al. Nitrogen-doped carbon nanotubes: growth, mechanism and structure. ChemPhysChem 2011;12:2995–3001, http://dx.doi.org/10.1002/cphc.201100454.
[38] Gao Z, Bandosz TJ, Zhao Z, Han M, Qiu J. Investigation of factors affecting adsorption of transition metals on oxidized carbon nanotubes. J Hazard Mater 2009;167:357–65, http://dx.doi.org/10.1016/j.jhazmat.2009.01.050.
[39] Fanning PE, Vannice MA. A DRIFTS study of the formation of surface groups on carbon by oxidation. Carbon 1993;31:721–30, http://dx.doi.org/10.1016/0008-6223(93)90009-Y.
[40] Misra A, Tyagi PK, Singh MK, Misra DS. FTIR studies of nitrogen doped carbon nanotubes. Diam Relat Mater 2006;15:385–8, http://dx.doi.org/10.1016/j.diamond.2005.08.013.
[41] Ferhat-Hamida Z, Barbier J Jr, Labruquere S, Duprez D. The chemical state of palladium in alkene and acetylene oxidation: a study by XRD, electron microscopy and TD-DTG analysis | Request PDF. Appl Catal B Environ 2001;29:195–205.
[42] Milonjić SK. A consideration of the correct calculation of thermodynamic parameters of adsorption. J Serb Chem Soc 2007;72:1363–7, http://dx.doi.org/10.2298/JSC0712363M.
[43] Vanyorek L, Prekob Á, Sikora E, Reizer E, Muránszky G, Kristály F, et al. Application of carbon nanotube coated aluminosilicate beads as "support on support" catalyst for hydrogenation of nitrobenzene. J Ind Eng Chem 2019;79:307–13, http://dx.doi.org/10.1016/j.jiec.2019.07.006.